

Two-Dimensional Antiferromagnetic Excitations from a Large Single Crystal of $\text{YBa}_2\text{Cu}_3\text{O}_{6.2}$

M. Sato^(a) and S. Shamoto

Institute for Molecular Science, Okazaki 444, Japan

J. M. Tranquada and G. Shirane

Brookhaven National Laboratory, Upton, New York 11973

and

B. Keimer^(a)

*Center for Materials Science and Engineering, Massachusetts Institute of Technology,
Cambridge, Massachusetts 02139*

(Received 3 June 1988)

A large single crystal ($7 \times 7 \times 3 \text{ mm}^3$) of $\text{YBa}_2\text{Cu}_3\text{O}_{6.2}$ has been grown and its magnetic excitations have been observed by neutron-scattering techniques. A two-dimensional magnetic ridge, similar to that observed for $\text{La}_2\text{CuO}_{4-y}$, has been clearly identified by triple-axis measurements. The slope of the dispersion curve for spin-wave excitations is very large ($\geq 0.5 \text{ eV \AA}$), consistent with the result of spin-pair Raman scattering by Lyons *et al.*

PACS numbers: 75.30.Ds, 74.70.Vy, 75.50.Ee

Spin correlations in the high- T_c superconductor system¹ $\text{La}_{2-x}\text{Sr}_x\text{CuO}_{4-y}$ have been very extensively investigated by neutron-scattering techniques.^{2,3} A novel type of two-dimensional (2D) antiferromagnetism was revealed in $\text{La}_2\text{CuO}_{4-y}$ above the 3D ordering temperature. Upon doping with Sr, both the Néel temperature and the spin-spin correlation length decrease rapidly. The correlation length drops to approximately 10 \AA at $x \approx 0.1$, where superconductivity sets in. However, the integrated intensity of the scattering from the correlated spins is roughly independent of doping, suggesting that the Cu magnetic moment is unchanged by doping and that it persists into the superconductive compositions.³

Similar two-dimensional magnetism is expected in the layered, perovskitelike system $\text{YBa}_2\text{Cu}_3\text{O}_{6+x}$, the second family of high-temperature superconductors to be discovered.⁴ The existence of long-range magnetic order in the nonsuperconducting members of this series ($x \lesssim 0.4$) was first established by muon-spin-rotation studies.⁵ The antiferromagnetic structure determined by powder neutron diffraction⁶ is shown in Fig. 1(a). The spin arrangement within a CuO_2 layer is identical to that found in $\text{La}_2\text{CuO}_{4-y}$.⁷ The Néel temperature, which is approximately 500 K for $x \approx 0$, decreases gradually with increasing oxygen content and then drops quickly to zero near $x \approx 0.4$.^{5,6} Lyons *et al.*⁸ have reported inelastic light-scattering measurements which, for a sample with $x \approx 0.0$, show a peak at 2600 cm^{-1} , from which a nearest-neighbor, antiferromagnetic exchange energy of $J \approx 950 \text{ cm}^{-1}$ is derived, corresponding to a zone-center spin-wave velocity of 0.64 eV \AA within the basal plane. They also observed that the spin-pair peak persists for the superconducting compositions $x \approx 0.6$ and 0.9 , although the peak is broadened and weakened and its

center of gravity moves to lower frequency. In this paper, we report the successful observation of two-dimensional spin-wave excitations from a large single crystal of $\text{YBa}_2\text{Cu}_3\text{O}_{6.2}$.

The study of spin dynamics in $\text{YBa}_2\text{Cu}_3\text{O}_{6+x}$ by inelastic neutron scattering has been prevented, up until very recently, by the unavailability of sufficiently large

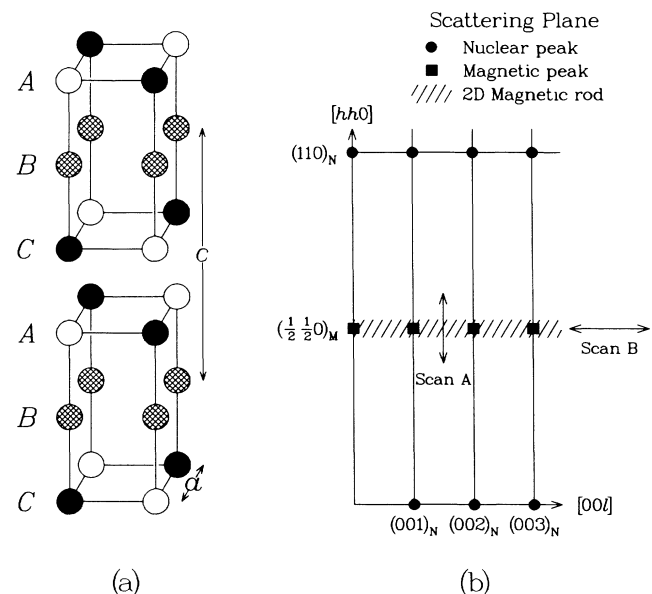


FIG. 1. (a) Magnetic spin arrangements in $\text{YBa}_2\text{Cu}_3\text{O}_{6+x}$ with x near zero. Cross-hatched circles represent nonmagnetic Cu^{1+} ions, while filled and open circles indicate antiparallel spins at Cu^{2+} sites. (b) Reciprocal-space (hkl) zone. The hatched line along $(\frac{1}{2}, \frac{1}{2}, l)$ is the magnetic ridge and A and B indicates scans shown in Figs. 2 and 3.

single-crystal specimens. The well-shaped, excellent-quality single crystals which have been used to study the anisotropy of various properties by many groups⁹ are, unfortunately, too small for our purposes; crystals of this type are typically no larger than $2 \times 2 \times 0.5 \text{ mm}^3$.¹⁰ However, it has been found that a much larger type of crystal, embedded in an ingot together with other crystals and residues of the crystal growth flux, can be grown. An "ingot crystal" similar to this second type was recently utilized by Kadowaki *et al.*¹¹ in a successful single-crystal diffraction study of a second type of antiferromagnetic ordering which occurs at low temperatures for $x \approx 0.35$.

For the present experiment, we have examined a total of nine ingot crystals with sizes in the range $0.2\text{--}0.4 \text{ cm}^3$. The crystals were grown from a mixture containing an excess of BaO and CuO.¹² All contained relatively large crystals; however, the first eight were rejected because of either too wide a mosaic ($> 4^\circ$) or too large a fraction of impurity phases. The last one (designated IMS No. 9) shows a relatively narrow mosaic of 1.2° and a tolerable level of impurity powder lines, mostly attributable to BaCuO_2 . To reduce the oxygen content and obtain an antiferromagnetic sample, the crystal was annealed in Ar at 700°C for two days. An accurate determination of the lattice constant at room temperature ($a = 3.863 \text{ \AA}$, $c = 11.823 \text{ \AA}$) together with the observation of a sharp transition at $T_N = 370 \text{ K}$ are consistent with an oxygen content of $x \approx 0.2$. No evidence of the second type of ordering by Kadowaki *et al.*¹¹ was observed down to 5 K . A very rough estimate of the size of the single crystal was made by comparison of the spin-wave intensities of this crystal to those of a $0.5\text{-cm}^3 \text{ La}_2\text{CuO}_{4-y}$ single crystal. Consulting Polaroid photographs of Bragg reflections, we conclude that crystal No. 9 is approximately $7 \times 7 \times 3 \text{ mm}^3$ in size.

A scattering experiment performed with this type of crystal requires special care and patience. Once it is established that only one large crystal is present, a small amount of impurity scattering can be tolerated as its main effect on inelastic triple-axis measurements is to increase the background. As shown in Fig. 2, well defined magnetic excitations are observed. Before discussing the inelastic measurements further, it may be helpful to first describe the expected form of the scattering. When strong spin correlations exist within 2D layers but not between them, as in the paramagnetic phase of $\text{La}_2\text{CuO}_{4-y}$, the magnetic scattering forms rods in reciprocal space in the direction perpendicular to the layers.² When 3D ordering occurs, the relatively weak coupling between CuO_2 planes has little effect on the inelastic part of the magnetic scattering and the rods evolve into spin-wave ridges, with very little dispersion along the ridge direction. Quasielastic two-axis scans provide an elegant way in which to integrate over energy transfers in 2D systems, allowing a straightforward

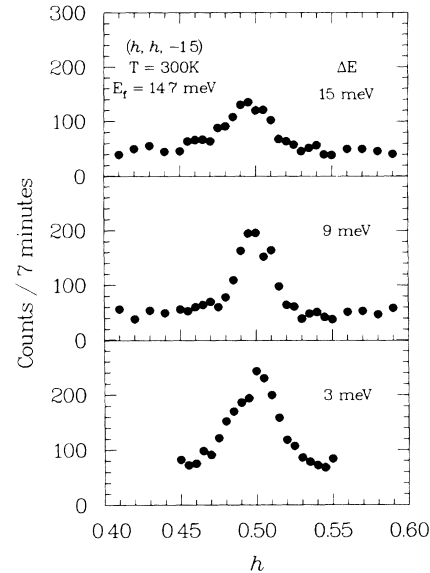


FIG. 2. Several constant- ΔE scans across the 2D magnetic ridge as indicated by scan *A* in Fig. 1(b). The zone center for 2D spin waves is along $(\frac{1}{2}, \frac{1}{2}, l)$. The normalization of the data to incident flux has been adjusted to take into account the presence of higher-energy harmonics in the incident beam.

determination of the 2D magnetic correlation length²; however, the elastic contribution from impurity powder lines made such measurements extremely difficult. In this Letter, we concentrate on the triple-axis study at 300 K .

Figure 2 depicts typical constant-energy-transfer, ΔE , scans [cf. scan *A* in Fig. 1(b)] across the two-dimensional ridge at $(\frac{1}{2}, \frac{1}{2}, -\frac{3}{2})$. The measurements were carried out at the High Flux Beam Reactor at Brookhaven with a final neutron energy of 14.7 meV at $40^\circ\text{--}40^\circ\text{--}80^\circ$ collimations. Since the Néel temperature is 370 K , the room-temperature data in Fig. 2 are well within the spin-wave regime; however, as in $\text{La}_2\text{CuO}_{4-y}$,² the slope of the dispersion curve is so steep that we could not resolve the $+|q|$ and $-|q|$ branches. [The zone center for 2D spin waves should be the rod $(\frac{1}{2}, \frac{1}{2}, l)$.] These constant- ΔE scans show very sharp profiles up to 15-meV energy transfer. Determination of the spin-wave velocity from the data is somewhat simpler than in the case of $\text{La}_2\text{CuO}_{4-y}$, where the small orthorhombic distortion of 1.5% , combined with twinning, creates double ridges.² A series of model calculations taking into account the spectrometer resolution function gives a lower limit for the spin-wave velocity of 0.5 eV \AA , which is quite consistent with the light-scattering results.⁸

When we surveyed the intensity along the ridge [cf. scan *B* in Fig. 1(b)], we discovered, to our surprise the systematic intensity variation shown in Fig. 3. This modulation was not present in $\text{La}_2\text{CuO}_{4-y}$ and is, of

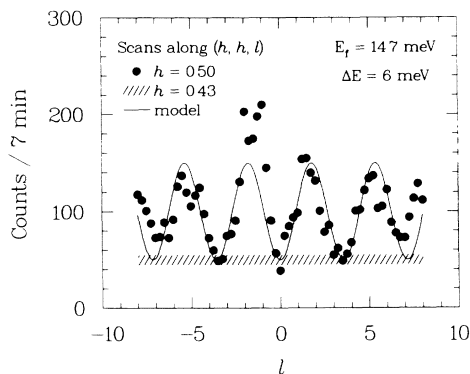


FIG. 3. Intensity variations along the magnetic ridge ($\frac{1}{2} \frac{1}{2} l$), caused by three-dimensional stacking of CuO_2 layers in a non-Bravais lattice. The solid line represents the square of the inelastic magnetic structure factor, G_M , which is given by Eq. (3).

course, caused by the three-dimensional stacking of CuO_2 layers, as shown in Fig. 1(a). We did not appreciate this intensity variation at the start of the experiment, and, hence, we took most of the data at small l values where the intensity is quite weak. This intensity modulation along the ridge is one of the important differences between La_2CuO_4 and $\text{YBa}_2\text{Cu}_3\text{O}_{6+x}$.

The differential cross section for spin-wave scattering involves a sum over correlations between spins on different sites:

$$\frac{d^2\sigma}{d\Omega dE} \sim \sum_{m,n} e^{i\mathbf{Q}\cdot(\mathbf{R}_m - \mathbf{R}_n)} \langle \hat{S}_m^a \hat{S}_n^a \rangle, \quad (1)$$

where \hat{S}_m^a is the a th component of the spin operator for site m and \mathbf{Q} is the momentum transfer. Because the Cu^{2+} ions in $\text{YBa}_2\text{Cu}_3\text{O}_{6+x}$ do not form a simple Bravais lattice, the phase factors do not all contribute simple factors of ± 1 . It also follows that, as for phonons in a lattice with a basis, the spin-wave modes should be split into optical and acoustic modes. A simple analysis then indicates that the intensity due to scattering from low-energy acoustic spin waves should be modulated by the square of an inelastic structure factor $G_M(\mathbf{Q})$ given by

$$G_M(\mathbf{Q}) = A(\mathbf{Q}_{\parallel}) \sin[\mathbf{Q}\cdot\boldsymbol{\rho} + \phi(\mathbf{q})], \quad (2)$$

where \mathbf{Q}_{\parallel} is the component of \mathbf{Q} parallel to the CuO_2 planes, $\phi(\mathbf{q})$ is a phase factor which depends on the eigenvectors, and the spin-wave wave vector is $\mathbf{q} = \mathbf{Q} - \boldsymbol{\tau}_M$, with $\boldsymbol{\tau}_M$ a reciprocal-lattice vector corresponding to a magnetic sublattice. The displacement vector $\boldsymbol{\rho}$ between nearest-neighbor CuO_2 planes has a magnitude cz' , where $z' = 1 - 2z$, and $z = 0.36$ is the fraction of a unit-cell length c by which the A and C layers are separated from B [see Fig. 1(a)]. The optical mode should have a cosine modulation with same phase. When $\mathbf{q} = 0$, $\phi(\mathbf{q})$ is equal to zero and the magnitude of $G_M(\mathbf{Q})$ is equal to that of the structure factor for mag-

netic Bragg reflections, as it must be.

We have evaluated the phase factor $\phi(\mathbf{q})$ in terms of a nearest-neighbor exchange model. Such a model requires three different exchange constants: J_{\parallel} within a CuO_2 plane, $J_{\perp 1}$ between nearest-neighbor A - C planes, and $J_{\perp 2}$ between next-nearest A - C planes. We know that $J_{\parallel} \gg J_{\perp 1}, J_{\perp 2}$; if we assume that $J_{\perp 1} \gg J_{\perp 2}$, then along the magnetic ridge ($\frac{1}{2} \frac{1}{2} l$) we find

$$G_M \approx A \sin(\pi z' l), \quad (3)$$

where l is continuous. Under these conditions it also follows that the cross section for the optical mode is much smaller than that for the acoustic. The solid curve in Fig. 3 represents G_M^2 of Eq. (3) offset by the background and scaled by an arbitrary amplitude factor. The intensity enhancement at $l \approx -1.5$ is probably due to the \mathbf{Q} dependence of the resolution function.

Observation of a single mode along the ridge with the $\sin^2(\pi z' l)$ intensity modulation tells us several things. First of all, it indicates that a spin-wave model should be appropriate for the analysis of magnetic excitations in the ordered phase. Next, the fact that only the acoustic mode is observed indicates that the coupling within CuO_2 bilayers is much stronger than the coupling between bilayers. Finally, the modulation is a clear signal that the peaks shown in Fig. 2 are indeed due to 2D spin waves within the CuO_2 layers.

We have now established that the antiferromagnetism in tetragonal $\text{YBa}_2\text{Cu}_3\text{O}_{6+x}$ is dominated by 2D interactions with a very strong coupling J_{\parallel} . This was expected; nevertheless it is very satisfying to see this expectation fully realized. Now the vital question is whether or not the magnetic correlations persist into the superconducting compositions beyond $x \approx 0.4$. Crystals in this range are now being prepared and exploratory neutron experiments are under way.

We would like to thank J. D. Axe, R. J. Birgeneau, V. J. Emery, and S. K. Sinha for very stimulating discussions. This work was supported by the U.S.-Japan Cooperative Neutron Scattering Program and a Grant-In-Aid for Special Project Research from the Japanese Ministry of Education, Science and Culture. Research at Brookhaven National Laboratory is supported by the Division of Materials Sciences, U.S. Department of Energy, under Contract No. DE-AC02-76CH00016. Work at the Massachusetts Institute of Technology is supported by the National Science Foundation under Contracts No. DMR85-01856 and No. DMR84-18718.

(a) Guest Scientist at Brookhaven National Laboratory, Upton, NY 11973.

¹J. G. Bednorz and K. A. Müller, *Z. Phys. B* **64**, 189 (1986).

²G. Shirane, Y. Endoh, R. J. Birgeneau, M. A. Kastner, Y. Hidaka, M. Oda, M. Suzuki, and T. Murakami, *Phys. Rev.*

Lett. **59**, 1613 (1987); Y. Endoh *et al.*, Phys. Rev. B **37**, 7443 (1988).

³R. J. Birgeneau *et al.*, unpublished.

⁴M. K. Wu *et al.*, Phys. Rev. Lett. **58**, 908 (1987).

⁵N. Nishida *et al.*, Jpn. J. Appl. Phys. **26**, L1856 (1987); J. H. Brewer *et al.*, Phys. Rev. Lett. **60**, 1073 (1988).

⁶J. M. Tranquada *et al.*, Phys. Rev. Lett. **60**, 156 (1988); J. M. Tranquada *et al.*, Phys. Rev. B **38**, 2477 (1988).

⁷D. Vaknin, S. K. Sinha, D. E. Moncton, D. C. Johnston, J. M. Newsam, C. R. Safinya, and H. E. King, Jr., Phys. Rev. Lett. **58**, 2802 (1987).

⁸K. B. Lyons, P. A. Fleury, L. F. Schneemeyer, and J. V. Waszczak, Phys. Rev. Lett. **60**, 732 (1988).

⁹For example, T. R. Dinger, T. K. Worthington, W. J. Gallagher, and R. L. Sandstrom, Phys. Rev. Lett. **58**, 2687 (1988).

¹⁰L. F. Schneemeyer *et al.*, Nature (London) **328**, 601 (1987).

¹¹H. Kadowaki, M. Nishi, Y. Yamada, H. Takeya, H. Takei, S. M. Shapiro, and G. Shirane, Phys. Rev. B **37**, 7932 (1988).

¹²Further details of the crystal growth technique are discussed in S. Shamoto, S. Hosoya, and M. Sato, Solid State Commun. **66**, 95 (1988).